

# The Effect of Baffles on Fluid Sloshing inside the Moving Rectangular Tank

Krit Threepopnartkul and Chakrit Suvanjumrat\*

Department of Mechanical Engineering, Faculty of Engineering, Mahidol University, Nakorn Pathom, Thailand 73170

## Abstract

Sloshing of fluid inside a container such as tanker trucks is the important phenomenon that develops pressure on tank wall which can cause structural damage or loss of the maneuvering stability. Decreasing the severe sloshing, the baffles are required to be included into the tank at appropriate locations. The FVM (Finite Volume Method) is the favorite method for analyzing the fluid sloshing. The effect of baffles on the fluid sloshing can be investigated using the computational models. This research improved C++ code of the fluid sloshing inside the movable tanks with and without baffles. These codes were implemented in the Open Source software that was the OpenFOAM. The computational results were validated with the experiment results which had a good correlation. The different results between simulation and experiment were digitized using the image processing techniques and had the average error less than 3.73%. This error can be proved that the computational method can be used to evaluate the effects of the baffles to control the sloshing of fluid inside the tanker trucks..

**Keywords:** Sloshing, Tank, FVM, Baffles, OpenFOAM

## 1. Introduction

Because of the liquid sloshing, partially filled with liquid inside the tanker trucks can perform many troubles during transporting whether it is the structural damage or the maneuvering stability. The amplitude of liquid sloshing depended on the nature amplitude and frequency of the tank motion, liquid-fill depth, liquid properties and tank geometry [1]. Many researches attempted to describe the liquid sloshing phenomenon using computational methods there was the Computational Fluid Dynamics (CFD) methods [2-4]. The CFD method might be comprised of Finite Element Methods (FEM), Finite Difference Method (FDM) or Finite Volume Methods (FVM). Whole methods were compared in [5]. The FVM was extensively used to describe the liquid sloshing. The partially liquid sloshing inside the moving tank was complicated phenomenon to write the governing equation because of there was the non-conservative and multi-phase flow. Previous research, [6], we validated the FVM of the half liquid-filled sloshing inside a rectangular tank by implemented using C++ code in the Open Source Field Operation and Manipulation (OpenFOAM). For this research we studied more complicated FVM that was the addition of a baffle inside the tank. The effect of a baffle would be studied and the CFD results would be used to be the patterns for reducing the severe sloshing of liquid inside tanks.

## 2. Mathematical models

The fluid flow was governed by Navier-Stokes equation [7]. For the multiphase flow, the aggregated fluid treated both phases of fluid as one aggregated fluid with varying properties and used one continuity and momentum equation for the mixture of both phases, whereas segregated fluid models used a continuity and momentum equation for each phase.

### 2.1 Continuity and Momentum Equations

The mass conservation was applied on an arbitrary part,  $\Omega$ , of the flow domain with the boundary,  $S$ , and

outward directed normal vector  $\vec{u}$ . The mass conservative equation was given by

$$\int_{\Omega} \frac{\partial \rho}{\partial t} d\Omega + \oint_S (\rho \vec{u}) \cdot \vec{n} dS = 0 \quad (1)$$

where  $\vec{u}$  was velocity and  $\rho$  was density.

By applied the gauss' divergence theorem, the integrate over  $S = d\Omega$  could be written as the integral over the volume,  $\Omega$ . Therefore, mass conservation could also be written in the conservative partial differential form as

$$\frac{\partial \rho}{\partial t} + \nabla \cdot (\rho \vec{u}) = 0 \quad (2)$$

or in the non-conservative notation form as

$$\frac{D\rho}{Dt} + \rho \nabla \cdot \vec{u} = 0 \quad (3)$$

When the velocity field was not divergence free ( $\nabla \cdot \vec{u} \neq 0$ ) this would result in a varying density for compressible flow. For incompressible flow the velocity field was always divergence free ( $\nabla \cdot \vec{u} = 0$ ). Similar to the mass conservation equation, the momentum equation was applied to a part  $\Omega$  of the flow domain with boundary  $S$ . It was given by

$$\int_{\Omega} \frac{\partial(\rho \vec{u})}{\partial t} d\Omega + \oint_S \rho \vec{u} (\vec{u} \cdot \vec{n}) dS + \oint_S p \vec{n} dS - \oint_S [\mu(\nabla \vec{u} + \nabla \vec{u}^T) - \frac{2}{3} \mu \nabla \cdot \vec{u}] \vec{n} dS - \int_{\Omega} \rho \vec{F} d\Omega = 0 \quad (4)$$

where  $p$  was pressure,  $\mu$  was dynamic viscosity and  $\vec{F}$  was external force, respectively. The terms in momentum equation were characterized as the time derivative, the convective term, the pressure gradient, the viscous term and the body force term. By applying Gauss' theorem, also the momentum equation could be written in the conservative divergence form as

$$\frac{\partial(\rho \vec{u})}{\partial t} + \nabla \cdot (\rho \vec{u} \vec{u}) + \nabla p - \nabla \cdot [\mu(\nabla \vec{u} + \nabla \vec{u}^T) - \frac{2}{3} \mu \nabla \cdot \vec{u}] - \rho \vec{F} = 0 \quad (5)$$

\* Corresponding Author: chakrit.suv@mahidol.ac.th, Telephone 662 889 2138 ext 6416, Fax. 662 889 2138 ext. 6429

The non-conservative form of the momentum equation was obtained by substituting the continuity, Eq. (2), into the momentum, Eq. (5), equation.

$$\rho \frac{\partial \bar{u}}{\partial t} + \bar{u} \frac{\partial \rho}{\partial t} + \rho(\bar{u} \cdot \nabla) \bar{u} + \bar{u} \nabla \cdot (\rho \bar{u}) + \nabla p - \nabla \cdot [\mu(\nabla \bar{u} + \nabla \bar{u}^T) - \frac{2}{3} \mu \nabla \cdot \bar{u}] - \rho \bar{F} = 0 \quad (6)$$

After dividing the remaining terms in the momentum Eq. (6) by the density, the continuity and non-conservative momentum equation were given by

$$\begin{aligned} \frac{\partial \rho}{\partial t} + \nabla \cdot (\rho \bar{u}) &= 0 & (7) \\ \frac{\partial \bar{u}}{\partial t} + (\bar{u} \cdot \nabla) \bar{u} + \frac{1}{\rho} \nabla p - \frac{1}{\rho} \nabla \cdot [\mu(\nabla \bar{u} + \nabla \bar{u}^T) - \frac{2}{3} \mu \nabla \cdot \bar{u}] - \bar{F} &= 0 & (8) \end{aligned}$$

## 2.2. Free surface equation

The volume of fluid (VOF) method, [8], was solved for one momentum equation and one continuity equation. These equations were the same for two phases. The physical properties of one fluid were calculated as weighted averages base on the volume fraction of the two fluids in one cell. The VOF in a cell was computed as

$$F_{vol} = \gamma V_{cell} \quad (9)$$

where  $V_{cell}$  was the volume of a computational cell and  $\gamma$  was the fluid fraction in a cell. The values of  $\gamma$  in a cell should be ranged between 0 and 1. If the cell was completely filled with fluid then  $\gamma=1$  and if it was filled with the void phase then its value should be 0. At the interface, the value of  $\gamma$  was between 0 and 1. The scalar function  $\gamma$  could be computed from a separate transport equation that taken the form as

$$\frac{D\gamma}{Dt} = \frac{\partial \gamma}{\partial t} + \nabla \cdot (\gamma \bar{u}) = 0 \quad (10)$$

The necessary compression of the surface was achieved by introducing an extra artificial compression term into the VOF equation as follow:

$$\frac{D\gamma}{Dt} = \frac{\partial \gamma}{\partial t} + \nabla \cdot (\gamma \bar{u}) + \nabla \cdot (\gamma(1-\gamma) \bar{u}_\gamma) = 0 \quad (11)$$

where  $\bar{u}_\gamma$  was a velocity field suitable to compress the interface. This artificial term was active only in the interface region due to the term  $\gamma(1-\gamma)$ .

The density,  $\rho$ , at any point in the domain was calculated as a weighted average of the volume fraction of the two fluids,  $\gamma$ , as

$$\rho = \gamma \rho_1 + (1-\gamma) \rho_2 \quad (12)$$

The surface tension force,  $F_s$ , which takes place only at the free surface, was computed as

$$F_s = \sigma K(x) \bar{n} \quad (13)$$

where  $\bar{n}$  was a unit vector normal to the interface that could be calculated from

$$\bar{n} = \frac{\nabla \gamma}{|\nabla \gamma|} \quad (14)$$

and  $K(x)$  was the curvature of the interface that could be calculated from

$$K(x) = \nabla \cdot \bar{n} \quad (15)$$

## 2.3 The motion equations

The movement of the control volume could be estimated by solving the external force,

$$\bar{F} = \frac{D(m\bar{u})}{Dt} \quad (16)$$

where  $m$  was the mass of the control volume

The velocity in every equation was the relative velocity which referenced to the moving coordinate and relative to the fix coordinate as shown in Fig.1

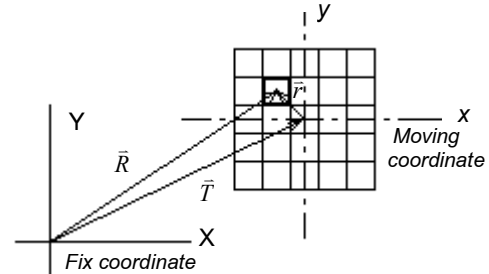


Fig. 1 The relation of the moving coordinate in the fix coordinates.

The motion of the rectangular tank was a direct consequence of the flow induced forces acting on its wall. The evaluation of 1-DOF motions was applied to the entire control volume which comprised sinusoidal translation as

$$T = A \left[ \sin \left( \frac{2\pi}{T_p} t + \phi \right) \right] \quad (17)$$

where  $T$  was the translation of a tank or the entire control volume,  $T_p$  was the translation period and  $\phi$  was the translation phase

## 3. Experiment Setup

The research methodology comprised of the experimental and numerical methods of the fluid sloshing. The experimental setup had been developed to investigate the surface wave and displacement of liquid (water) as shown in Fig.2. The clear acrylic rectangular tank without baffle had dimension of 300×240×50 mm (width×height×depth). The tank with baffle had same dimension as the tank without baffle. A baffle had dimension of 50×120 mm (depth× height) and installed at middle of the width of the tank. The water-filled inside the tank at three levels that are 1/4, 1/2 and 3/4 of the tank volumes. The motion of the partially water filled tanks (all of levels of water) were controlled by the servo motor and the ball screw with velocity of 200, 300 and 400 mm/s, respectively. The velocity and position of the tank were controlled by voltage supplied to the servo motor. The input voltage controlled the time function of position for this experiment as shown by graph in Fig.3. The water sloshing inside the tank would be carried out using a Logitech webcam, model "Quickcam Pro for Notebook" which moved with the tanks and connected to a computer via a USB port.

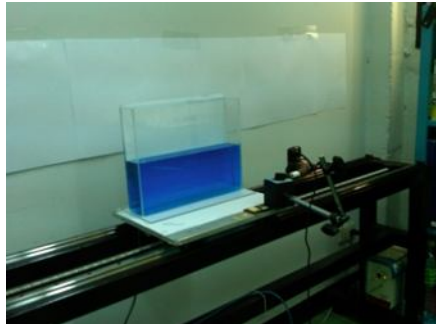


Fig. 2 Apparatus of experimental device for sloshing

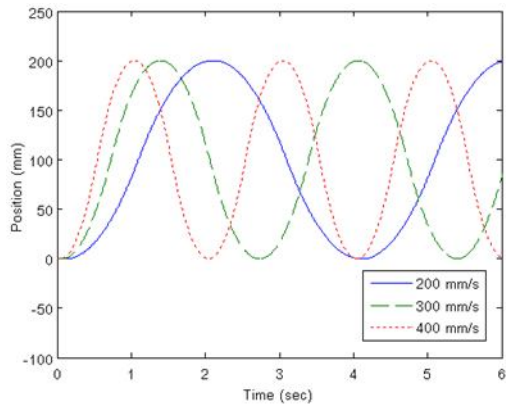


Fig. 3 The input signals to control the position of the rectangular tanks.

The governing Eqs. (1) – (17) were discretized and implemented using C++ language in three dimensions space of OpenFOAM. The 1,920 small parallelepiped control volumes were created and combined to be the tank which dimension is 300×240×50 mm (width×height×depth) as shown in Fig.4a. The 1,920 small parallelepiped control volume were also created and combined to be the tank with a baffle had dimension 50×120 mm (depth× height) as shown in Fig.4b.

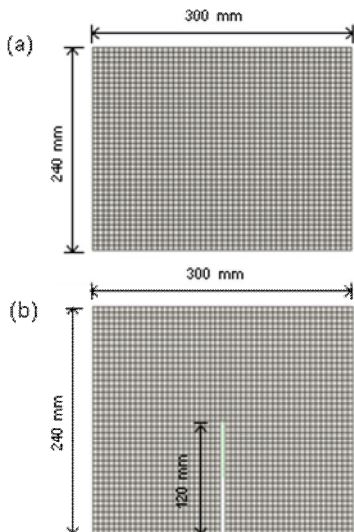


Fig.4 (a) FV model of the tank without baffles and (b) FV model of the tank with a baffle.

The volume of water at initial condition ( $t=0$ ) performed by selecting cells to fill water and defined  $\gamma$  in Eq. (12) to be unity for these cells. The computer graphic of the initial condition of the partially water-filled were shown in Fig. 5. The red and blue color-filled in cells instead water and air, respectively. For solving the pressure and velocity of fluid inside the moving tank, the Pressure Implicit with Splitting of Operators (PISO) algorithm was used in this research. The laptop (specification: Pentium Core™2 Duo E7500-2.93 GHz and 2.0 GB RAM) was used for the simulated process.

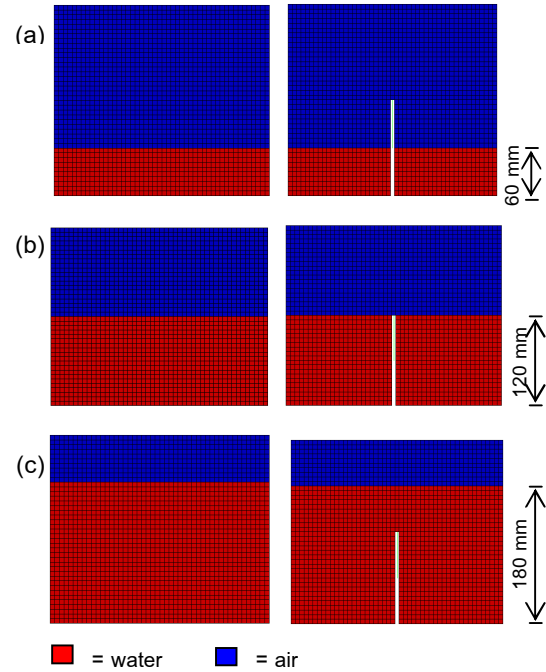


Fig. 5 The initial conditions for the FV models of the tanks with and without a baffle when the water-filled were (a) 1/4, (b) 1/2 and (c) 3/4 of tank volumes.

#### 4. Results and Discussion

The tanks were controlled to move back and forth from left to right with velocity of 200, 300, 400 mm/s and positions according to the input signals (Fig. 3). The water sloshing inside the moving tank was recorded. Examples of the image series for the surface wave of the water-filled 1/2 of the tank volume for the tank with and without baffle moving 400 mm/s were shown in Fig.6. The height of surface wave developed on the wall of the tank with a baffle expressed that the baffle could reduce the severe of the surface wave when compared the image of the height of the surface wave on the wall of the tank without baffle.

The computational results were displayed using the third-party Open Source Software (ParaView) of OpenFOAM which could convert the numerical results to the graphic results. The image series of the FVM at the same time of the experiment were shown in Fig.7. The surface of water inside both tanks. (with and without a baffle) had a good correlated movement when compared with the surface wave of the experiments.

The sequences of the surface wave could express the maximum height of the sloshing water inside the rectangular tank which moved from the left to the right. The height of the surface wave at the tank wall would lift up and fall down corresponding to the movement of the tank.

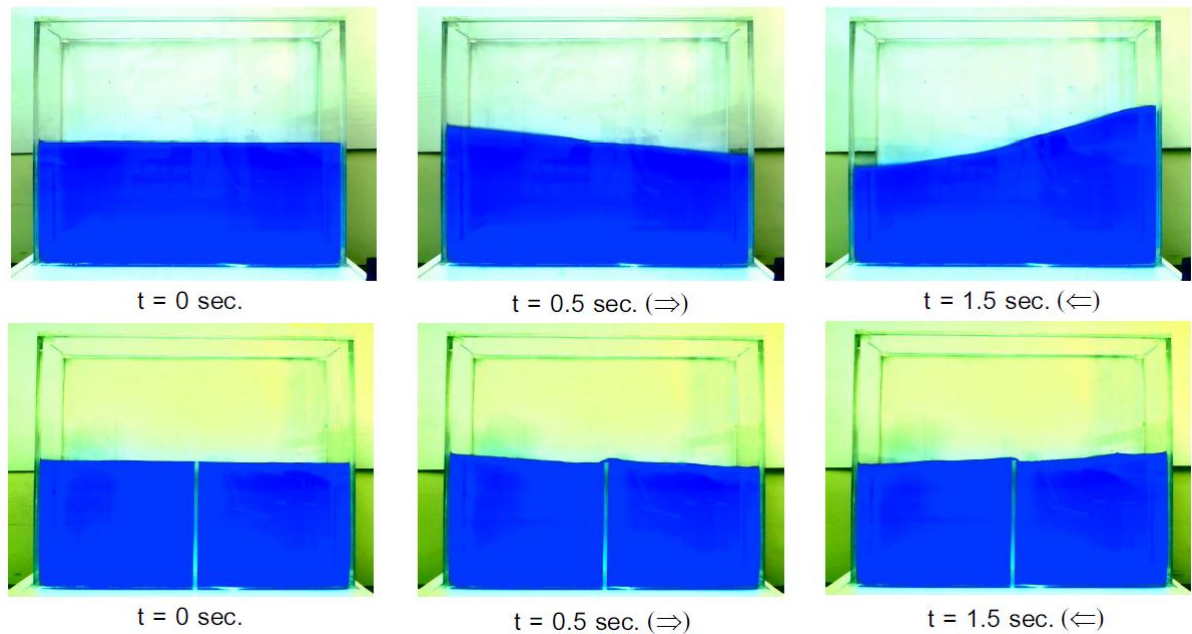


Fig. 6. Sequential images of the experimental surface wave inside the tank with and without a baffle at the initial condition and move to right ( $\Rightarrow$ ) and left ( $\Leftarrow$ ), respectively.

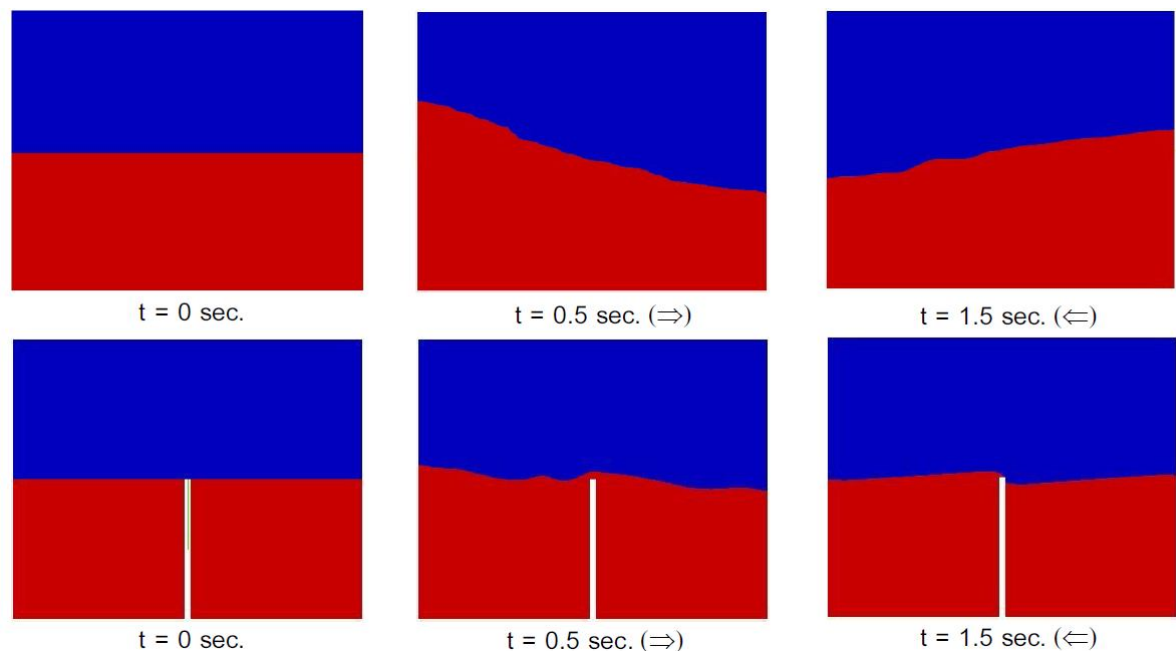


Fig. 7. Sequential images of the FVM surface wave inside the tank with and without a baffle at the initial condition and move to right ( $\Rightarrow$ ) and left ( $\Leftarrow$ ), respectively.

The “SloshDetector” software, [9], was used to determine the coordinates of the surface wave height at the left wall of tank. The variable heights of the surface wave on the left wall of tank could be plotted to compare between CFD and experimental results as shown in Figs. 8-13. The average error of the CFD when compared with the experiment results for the volume of water were 1/4, 1/2 and 3/4 of the tanks for every velocity of the tanks movement were 6.22%, 2.67% and 2.29%, respectively. Graphs in Figs. 8-10 shown for increasing of water levels and velocities of tank movements directly affected to the sloshing phenomena which had the severe sloshing. Decreasing the violent sloshing, a baffle was required to be installed into the tank. The effects of a baffle for reducing the severe sloshing were shown in Figs. 11-13. The comparisons of the maximum surface heights on the left wall of the tank with and without a baffle were described in Table. 1. The free surface height at the same levels of the baffle height had excellent results for every velocity of the tank movements.

## 5. Conclusion

The FVM technique for the multi phases flow had been used to simulate partially liquid sloshing in the moving rectangular tank with and without a baffle. The average error of 3.73% when comparing CFD to experimental results confirmed the good performance of FVM. The liquid sloshing on a baffle of tank exhibited the prominent behavior that the displacements of free surface wave were decreased and become linearity. The appropriated levels of water inside the tanks were equal the height of a baffles. The shallow water flow across the tip of a baffle during tank moved from the left to right cause the most reducing of the severed sloshing.

These effects of baffle that received from the experiment and FVM results for the liquid sloshing were the good study case. Furthermore, the FVM in OpenFOAM software would be used to design the good efficiency baffles inside tank.

Table.1 Max. different height of the wave surface in the tanks with and without a baffle

Initial surface height (mm)	Velocity of tanks (mm/s)	Different height between the wave surface and initial surface.	
		Tank without baffles (mm)	Tank with a baffle (mm)
60	200	14.62	5.81
	300	21.37	6.45
	400	32.84	11.81
120	200	5.00	2.7
	300	11.45	4.4
	400	68.71	5.5
180	200	7.55	5.85
	300	7.91	11.22
	400	47.68	27.55

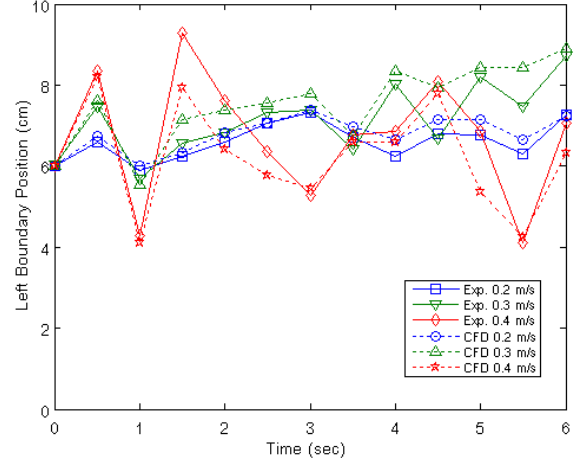


Fig. 8 Plot of the surface heights on the left wall of tank without baffle vs. time comparing CFD to experiments of the water 1/4 tank volume.

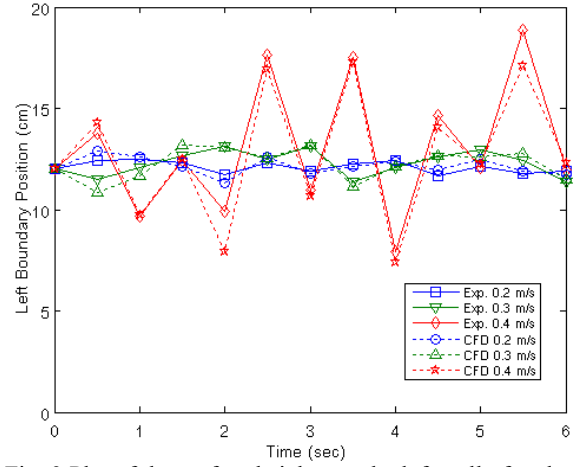


Fig. 9 Plot of the surface heights on the left wall of tank without baffle vs. time comparing CFD to experiments of the water 1/2 tank volume.

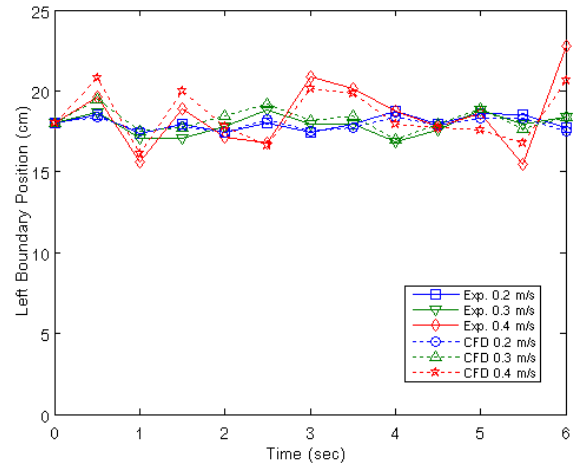


Fig. 10 Plot of the surface heights on the left wall of tank without baffle vs. time comparing CFD to experiments of the water 3/4 tank volume.

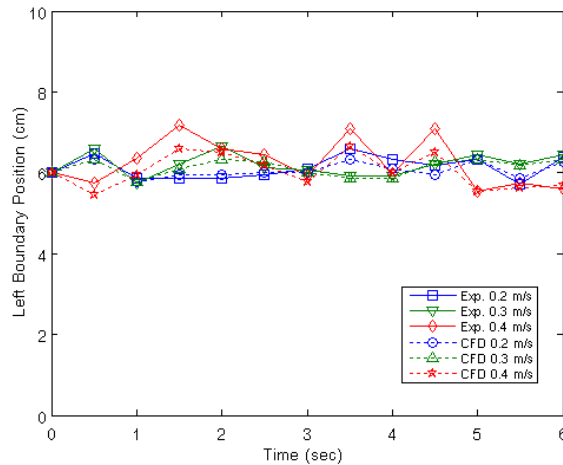


Fig. 11 Plot of the surface heights on the left wall of tank with baffle vs. time comparing CFD to experiments of the water 1/4 tank volume.

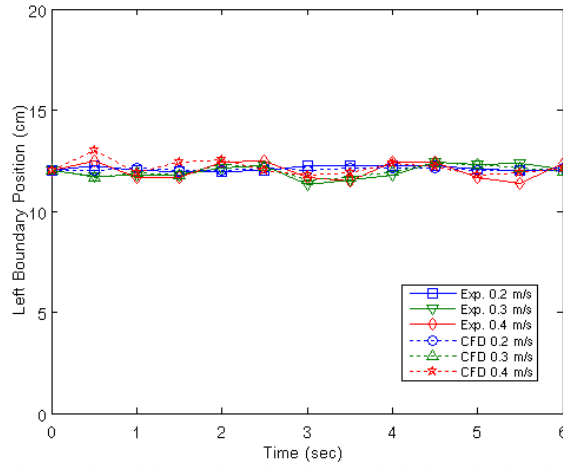


Fig. 12 Plot of the surface heights on the left wall of tank with baffle vs. time comparing CFD to experiments of the water 1/2 tank volume.

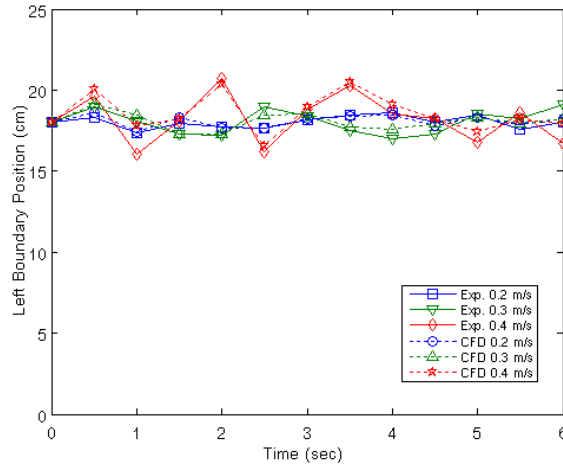


Fig. 13 Plot of the surface heights on the left wall of tank with baffle vs. time comparing CFD to experiments of the water 3/4 tank volume.

## 6. Acknowledgement

The authors wish to thank Asst. Prof. Tumrong Puttapitukporn on the used of the experimental devices at Mechanical Engineering Department, Kasetsart University.

## 7. References

- [1] Akyildizan, H. and Erdem U.N. (2006). Sloshing in a three-dimensional rectangular tank: Numerical simulation and experimental validation, *Ocean Engineering*, vol. 33, March 2006, pp. 2135–2149.
- [2] Liu, D. and Lin, P. (2008). A numerical study of three-dimensional liquid sloshing in tanks, *Journal of Computational Physics*, vol. 227, December 2007, pp. 3921–3939.
- [3] Cho, J.R., Lee, H.W. and Ha, S.Y. (2005). Finite element analysis of resonant sloshing response in 2-D baffled tank, *Journal of Sound and vibration*, vol. 288, April 2005, pp. 829–845.
- [4] Eswaran, M., Saha U.K. and Maity, D. (2009). Effect of baffles on a partially filled cubic tank: Numerical simulation and experimental validation, *Computers and Structures*, vol. 87, December 2008, pp. 198–205.
- [5] Rebouillant, S. and Liksonov, D. (2010). Fluid-structure interaction in partially filled liquid container: A comparative review of numerical approaches, *Computers & Fluids*, vol. 39, January 2010, pp. 739–746.
- [6] Threepopnartkul, K. and Suvanjumrat, C. (2010). Development and validation of a C++ object oriented CFD codes for two dimensional fluid sloshing simulations, paper presented in *The 36<sup>th</sup> Congress on Science and Technology of Thailand*, Bangkok, Thailand.
- [7] Anderson Jr., J.D. (1995). Computational fluid Dynamics: The basics with applications, McGraw-Hill, New York.
- [8] Hirt, C.W. and Nichols, B.D. (1981). Volume of fluid (VOF) method for the dynamics of free boundaries, *Journal of Computational Physics*, vol. 39, November 1979, pp. 201–225.
- [9] Suvanjumrat, C. and Puttapitukporn, T. (2010). Sloshing surface monitoring using image processing, paper presented in *The first TSME International Conference on Mechanical Engineering*, Ubon Ratchathani, Thailand